

# MWQ: Multiscale Wavelet Quantized Neural Networks

Qigong Sun, Yan Ren, Licheng Jiao, Xiufang Li, Fanhua Shang, Fang Liu

Key Laboratory of Intelligent Perception and Image Understanding of Ministry of Education, International Research Center for Intelligent Perception and Computation, Joint International Research Laboratory of Intelligent Perception and Computation, School of Artificial Intelligence, Xidian University, Xi'an, Shaanxi Province 710071, China

xd.qigongsun@163.com, yanren@stu.xidian.edu.cn, lchjiao@mail.xidian.edu.cn, xfl\_xidian@163.com, fhshang@xidian.edu.cn, f63liu@163.com

## Abstract

Model quantization can reduce the model size and computational latency, it has become an essential technique for the deployment of deep neural networks on resource-constrained hardware (e.g., mobile phones and embedded devices). The existing quantization methods mainly consider the numerical elements of the weights and activation values, ignoring the relationship between elements. The decline of representation ability and information loss usually lead to the performance degradation. Inspired by the characteristics of images in the frequency domain, we propose a novel multiscale wavelet quantization (MWQ) method. This method decomposes original data into multiscale frequency components by wavelet transform, and then quantizes the components of different scales, respectively. It exploits the multiscale frequency and spatial information to alleviate the information loss caused by quantization in the spatial domain. Because of the flexibility of MWQ, we demonstrate three applications (e.g., model compression, quantized network optimization, and information enhancement) on the ImageNet and COCO datasets. Experimental results show that our method has stronger representation ability and can play an effective role in quantized neural networks.

## 1. Introduction

With the development of artificial intelligence, deep neural networks (DNNs) have achieved remarkable results in many fields, such as image recognition, natural language processing, and video analysis. When deeper networks are used to solve various problems, a lot of computing resources and memory are needed urgently. With the rapid development of chip technologies (e.g., GPU and TPU), the computing frequency and efficiency have been greatly improved. However, for low-power platforms (e.g., mobile phones, embedded devices, and smart chips) with limited resources, it is difficult to achieve satisfactory performance

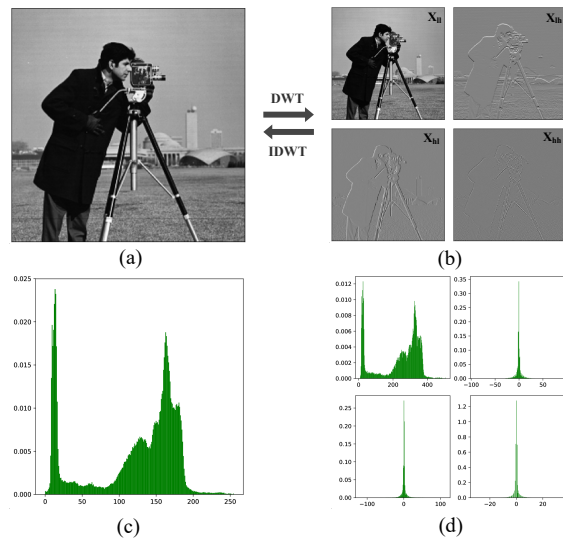


Figure 1: Image visualization and comparison of histograms. (a) Original image. (b) High and low frequency components after image decomposition. (c) Statistical distribution of original image. (d) Statistical distribution of various components in different frequencies after wavelet transform.

(e.g., power dissipation, speed and accuracy) in various industrial applications. Model quantization is a kind of model compression technology, which transforms the infinite continuous floating-point values into finite discrete fixed-point values. Recently, some smart chips support low-bit numerical computation, e.g., Apple A12 Bionic [10], Nvidia Turing GPU [37], BitFusion [40], and BISMO [45]. Compared with the full-precision model, the quantized model has less parameter storage, lower bandwidth requirements, faster computing speed, lower energy and memory consumption. Despite these attractive benefits, it inevitably leads to the deviation between original data and its quantized value. Especially when the data is quantized to extreme low-bit, the information loss will cause unstable training and severe performance degradation.

arXiv:2103.05363v1 [cs.CV] 9 Mar 2021

At present, almost all quantization methods directly quantize numerical elements of the weights and activation values, ignoring the relationship between elements. The decline of representation ability, the loss of information and inadequate training lead to the performance degradation of quantized neural networks. Spatial information (e.g., corners, edges, textures, and shapes) and multiscale frequency information play significant roles in image classification, object detection, semantic segmentation, and scene understanding. Wavelet [34, 6] is a powerful time–frequency analysis tool, which can be applied to decompose images into various components with different frequencies. Each component represents different scale information and spatial information. Fig. 1 shows the decomposition of image  $\mathbf{X}$  by *Haar* wavelet, and the histograms denote the data distributions before and after discrete wavelet transform (DWT). The low frequency component  $\mathbf{X}_{ll}$  is the down sampling of the original image, and the high frequency components  $\mathbf{X}_{lh}$ ,  $\mathbf{X}_{hl}$  and  $\mathbf{X}_{hh}$  contain more image details (e.g., corners, edges, textures, and shapes) in different directions. It can be seen from Fig. 1 that the different scale components with different distributions have obviously different frequency and spatial information. These information can not be considered by traditional spatial quantization methods, which lead to information loss and performance degradation.

Inspired by the characteristics of images in the frequency domain, we propose a novel multiscale wavelet quantization (MWQ) method. This method uses wavelet transform (e.g., DWT and IDWT) to decompose original data into multiscale components (which contain frequency and spatial information), and then matches the appropriate quantization parameters (e.g., range and step size) for each component. By adaptively quantizing each component, it can alleviate the information loss caused by traditional quantization and improve the performance of the quantized model. The advantages of our method are shown as follows:

- **Stronger representation ability.** Assuming that we quantize the weights to  $k$ -bit, the traditional quantizers can represent up to  $2^k$  states. For MWQ, quantization is applied in the frequency domain, and each frequency component can be quantized into  $2^k$  states. After IDWT reconstruction, the number of representation states can be significantly more than  $2^k$ . Therefore, MWQ has stronger representation ability than traditional quantizers, as shown in Fig. 6 in Section 4.1.
- **Multiscale quantization.** Wavelet transform can decompose original data to different scales through low pass filters and high pass filters. Different scale components contain different information with different distributions, as shown in Fig. 1. According to the data distribution in each frequency domain, we can clip the

data to a more suitable range for rounding to reduce the loss caused by quantization.

- **Spatial relevance.** Due to the existence of quantization receptive field, which is defined by the shape of the wavelet base, each element after wavelet transform is related to the spatial neighborhoods of original data. The proposed method not only considers the numerical value, but also integrates the spatial neighborhood information, as shown in Fig. 4.
- **Application flexibility.** Compared with the standard Fourier transform, wavelet transform shows diversity based on different wavelet bases. The commonly used wavelet bases are *Haar*, *Daubechies*, *Coiflet*, and *Symlets*. We can carry out wavelet decomposition with different wavelet base at different level, and then implement quantization with various quantizers according to different bit-width requirements. Because of the flexibility of MWQ, it can support a variety of applications (e.g., model compression, quantized network optimization, and information enhancement).
- **State-of-the-art results.** We apply the proposed techniques on image classification, object detection, and instance segmentation tasks. The experimental results show that our techniques are more effective than other counterparts under similar constraints.

## 2. Related works

### 2.1. Model Quantization

As one of the typical methods of model compression and acceleration, model quantization usually quantizes the full-precision parameters to low-bit. The commonly used quantizers can be categorized into three modalities: uniform quantizers (e.g., PACT [5], Dorefa-Net [54], QIL [19] and MBN [43]), logarithmic quantizers (e.g., LogQuant [36], INQ [53] and ShiftCNN [13]) and adaptive quantizers (e.g., AdaBits [18] and APoT [26]). Under extreme constraints, weights and activation values can also be quantized into binary (e.g., BNN [17], MBN [42] and XNOR-Net [38]) or ternary (e.g., TWN [21] and TTQ [55]), which can be computed by bitwise operations (e.g., `xnor`, and `bitcount`). Some studies [46, 49, 2, 41] show that mixed-precision quantization can achieve better performance according to the sensitivities of different layers. It is hardly to access the accurate gradients for discrete quantization, and the commonly used method is to resort to appropriate approximation. Straight through estimation (STE) [1, 11] uses the nonzero gradient to approximate the function gradient, which is not-differentiable or whose derivative is zero. When the values are quantized to extremely low-bit, STE greatly harms the performance of quantized models [22, 35]. DSQ [12]

employs a series of hyperbolic tangent functions to gradually approach the staircase function for low-bit quantization, which makes the forward and backward process more consistent and stable in the training. However, it can not be used to approximate the nonuniform quantization.

## 2.2. Wavelets

Wavelet is derived from multi-resolution analysis, and it expresses a function as a series of successive approximation components, and each component represents a different resolution. The commonly used wavelets include orthogonal wavelets, biorthogonal wavelets, multiwavelets, ridgelet, curvelets, bandelets, and contourlets, etc. This technique is often used for function approximation [52] and signal processing [33, 44]. The discrete wavelet transform (DWT) can be used to decompose an image into different levels of frequency interpretations, and the inverse discrete wavelet transform (IDWT) can reconstruct original image by using the multi-frequency components. In image processing, wavelet transform is often used as a tool for content information analysis [34]. With the development of DNNs, wavelet transform has several attempts to combine the classical signal processing and deep learning methods, such as image denoising [20, 31, 47], super resolution [16, 30], classification [7, 25, 29], segmentation [24], facial aging [32], style transfer [50], remote sensing image processing [9], etc. It is often used as the tool of data preprocessing, post-processing, feature extraction, and sampling operators in DNNs [16, 32, 39, 48, 30, 23]. [25] utilizes DWT to replace max-pooling, strided-convolution, and average-pooling to suppress the noise effect. Multi-level wavelet CNN [30] use DWT to concatenate the frequency and position information of feature mapping which preserve texture details. [32] incorporates a wavelet packet transform module to improve the visual fidelity of generated images by capturing age-related texture details at multiple scales in the frequency space.

## 3. Approach

In this paper, we innovatively view the model quantization from the perspective of the frequency domain. Through wavelet transform, multiscale frequency and spatial information are considered to alleviate the information loss and performance degradation caused by quantization. In this section, we first review the process of DWT and IDWT operations, and discuss the feasibility in DNNs. Then we analyze the problem of traditional quantizers and introduce our method in more detail.

### 3.1. DWT and IDWT Operations

Similar to Fourier series that use the combination of sine functions to represent a discrete signal, wavelet can decompose a signal in different frequency domains. DWT can decompose a signal into multiscale components with different

frequencies. After multi-level DWT, the original signal  $s$  can be mathematically represented by the summation of approximated version  $s^l$  and detailed versions  $s^h$  as defined below.

$$\mathbf{s} = \mathbf{s}_1^h \oplus \mathbf{s}_1^l = \mathbf{s}_1^h \oplus \mathbf{s}_2^h \oplus \cdots \oplus \mathbf{s}_n^h \oplus \mathbf{s}_n^l, \quad (1)$$

where  $n$  represents the decomposition level. Suppose  $\mathbf{s} = \{s[n]\}_{n \in [1, N]}$  is a 1D discrete signal. The DWT of this signal is calculated by passing it through a series of filters (e.g., low pass filter  $\mathbf{g} = \{g[k]\}$  and high pass filter  $\mathbf{h} = \{h[k]\}$ ). The first level low frequency component  $\mathbf{s}_1^l$  and high frequency component  $\mathbf{s}_1^h$  can be expressed as follows:

$$s_1^l[k] = \sum_j s[j]g[j - 2k], \quad (2)$$

$$s_1^h[k] = \sum_j s[j]h[j - 2k]. \quad (3)$$

IDWT can use the decomposed components to reconstruct the original signal as follows:

$$s[j] = \sum_k (s_1^l[k]g[j - 2k] + s_1^h[k]h[j - 2k]). \quad (4)$$

In image processing, the original image  $\mathbf{X}$  can be decomposed into one low frequency component  $\mathbf{X}_{ll}$  and three high frequency components  $\mathbf{X}_{lh}$ ,  $\mathbf{X}_{hl}$  and  $\mathbf{X}_{hh}$  by single-level DWT, where the low frequency component denotes the approximation coefficient and the high frequency components contain more image details (e.g., edges, shapes and textures). For a given image  $\mathbf{X} \in \mathbb{R}^{m \times n}$ , the DWT decomposition can be expressed as follows:

$$\mathbf{X}_{c_0 c_1} = (1 \downarrow 2)(\mathbf{f}_{c_1} \otimes_c (2 \downarrow 1)(\mathbf{f}_{c_0} \otimes_r \mathbf{X})), c_0, c_1 \in \{l, h\}, \quad (5)$$

where  $\otimes_r$  and  $\otimes_c$  denote the convolution for the rows and columns of the entry,  $(2 \downarrow 1)$  and  $(1 \downarrow 2)$  denote the down-sample columns and rows, respectively.  $\mathbf{f}_l$  and  $\mathbf{f}_h$  represent the low pass filter and high pass filter, which are determined by the wavelet base (e.g., *Haar* and *Daubechies*). Similar to DWT, various frequency components can also be used to reconstruct the original image as follows:

$$\mathbf{X} = \sum_{c_1} \mathbf{f}_{c_1} \otimes_r (2 \uparrow 1) \left( \sum_{c_0} \mathbf{f}_{c_0} \otimes_c (1 \uparrow 2) \mathbf{X}_{c_0 c_1} \right), \quad (6)$$

where  $c_0, c_1 \in \{l, h\}$ ,  $\otimes_r$  and  $\otimes_c$  denote the deconvolution for the rows and columns of the entry,  $(2 \uparrow 1)$  and  $(1 \uparrow 2)$  denote the upsample columns and rows, respectively.

Fig. 2 describes the basic decomposition and reconstruction steps for an image. In order to facilitate the application of wavelet transformation in DNNs, we use convolution and fractionally-strided convolution to implement DWT and IDWT operations in PyTorch. The low pass filter and high pass filter can be defined as convolution kernels. The convolution direction is controlled by the shape of convolution filter, and the upsample and downsample are controlled by stride. Therefore, DWT and IDWT can be used to participate in the forward and backward propagations of DNNs.

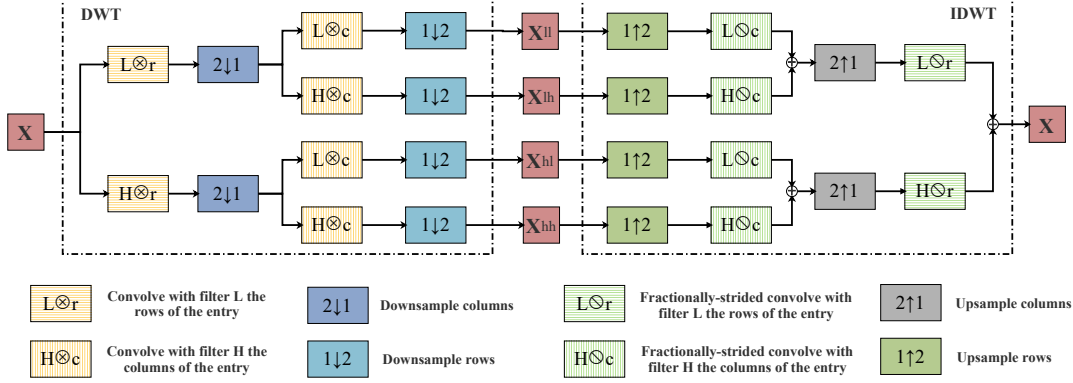


Figure 2: Illustration of DWT and IDWT for image data. The low-frequency component  $X_{ll}$  contains the main information of original image and the high-frequency components  $X_{lh}$ ,  $X_{hl}$  and  $X_{hh}$  denote the vertical, horizontal and diagonal components of image.

### 3.2. Traditional Quantizer

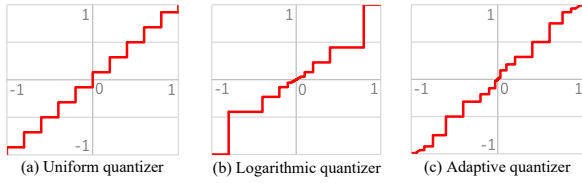


Figure 3: Schematic diagram of the three quantizers.

Model quantization is an effective model compression technique. For example, if we quantize the weights to 4-bit, we can achieve  $8\times$  of the model compression ratio. Suppose we use  $X^i$  and  $X^{i+1}$  to represent the input data and output data of the  $i$ -th layer.  $W^i$  denotes the weights, and  $\mathcal{F}()$  denotes the calculation operations (e.g., full connection or convolution). The calculation between two variables can be shown as follows:

$$X^{i+1} = \mathcal{F}(\hat{X}_n^i, \hat{W}_m^i) = \mathcal{F}(\mathcal{Q}(X^i, n), \mathcal{Q}(W^i, m)), \quad (7)$$

where  $\mathcal{Q}()$  denotes the quantizer, and  $n$  and  $m$  represent the bit-widths of input data and weights. The calculation of quantized variables ( $\hat{X}_n^i$  and  $\hat{W}_m^i$ ) can be accelerated by a special accelerator (e.g., BitFusion [40] and BISMO [45]). Fig. 3 shows the schematic diagram of uniform quantizer, logarithmic quantizer, and adaptive quantizer. Existing quantizers learn the range and step size of quantization by data distribution. They only focus on the numerical value and ignore the spatial information of the data. Therefore, it is easy to cause the loss of spatial information (e.g., edges, textures, and shapes) and severe performance degradation.

### 3.3. Multiscale Wavelet Quantization

In order to alleviate the information loss caused by quantization, we propose a novel multiscale wavelet quantization method based on the characteristics of wavelet transform. We use the DWT operation to decompose the original data into its multiscale frequency components. The decomposed components represent the mapping of the original data at different scales. Different components con-

tain different contents and have different distributions. Therefore, we can use the traditional quantizer (e.g., Uniform and APoT) to quantize each components separately to reduce the information loss. Finally, we reconstruct the quantized components by the IDWT operation to serve as network computing. The main process can be expressed as follows:

$$X_{ll}^i, X_{lh}^i, X_{hl}^i, X_{hh}^i = DWT(X^i, name, J), \quad (8)$$

$$\hat{X}_{c_0, c_1}^i = \mathcal{Q}(X_{c_0, c_1}^i, n), c_0, c_1 \in \{l, h\} \quad (9)$$

$$\hat{X}^i = IDWT(\hat{X}_{ll}^i, \hat{X}_{lh}^i, \hat{X}_{hl}^i, \hat{X}_{hh}^i, name, J) \quad (10)$$

where  $DWT()$  and  $IDWT()$  represent the DWT and IDWT operations defined in Section 3.1,  $name$  denotes the wavelet base (e.g., *Haar*, *Daubechies*, *Coiflet*, and *Symlets*), and  $J$  denotes the level of wavelet decomposition.  $\mathcal{Q}()$  denotes the quantizer, in which the quantization range and step size are different for different components.  $\hat{X}_{ll}^i$ ,  $\hat{X}_{lh}^i$ ,  $\hat{X}_{hl}^i$  and  $\hat{X}_{hh}^i$  are the quantized multiscale frequency components.

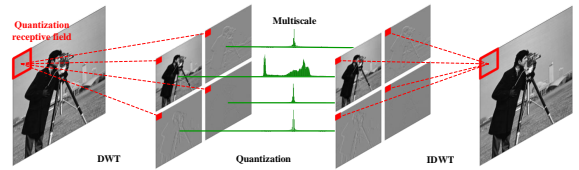


Figure 4: Schematic diagram of multiscale wavelet quantization.

In addition to considering the multiscale information in each frequency domain, our method also takes into account the spatial neighborhood information. Fig. 4 shows the schematic diagram of MWQ. Obviously, the low frequency component is the down sampling of the original data, which has a similar distribution as the original data. High frequency components mainly present the details of the original data. As can be seen from Fig. 4, each element (red unit) of the frequency component is derived from the spatial neighborhood (red block) of the original data. The block in the spatial domain is called **quantization recep-**

**tive field**, which is defined by the shape of the wavelet filter. For example, the quantization receptive fields of *Haar* and *Daubechies* are 2 and 4, respectively. Therefore, MWQ considers the correlation of spatial information and preserves the spatial information as much as possible.

#### 4. Applications and Experiments

MWQ can make use of the decomposed multiscale frequency information and spatial neighborhood information to alleviate the performance degradation caused by the quantization in the spatial domain. In order to verify the effectiveness of our proposed quantization method, we apply it to image classification, object detection and instance segmentation tasks. The first experiment is model compression, which only focuses on the quantization of weights. MWQ is applied on the weights, and the activation values are in full-precision form or quantized by traditional quantizers. Then we verify the effectiveness of our method in the optimization of the traditional quantized networks. Finally, we use the multiscale features of wavelet decomposition to enhance the high frequency component information, and verify the importance of spatial information (e.g., edges, textures, and shapes). The implementation details and experimental results are shown below.

**Quantizer:** We use the hardware friendly uniform quantization function as the quantizer for the following experiments. The  $m$ -bit quantization of weights  $\mathbf{W}^i$  can be formulated as follows:

$$\mathcal{Q}(\mathbf{W}^i, m) = \text{round}(\text{clamp}(\mathbf{W}^i/s^i, -1, 1) * S) * d^i, \quad (11)$$

*s.t.*  $S = 2^{m-1} - 1, \quad d^i = s^i/S,$

where the clamp function is used to truncate all values into the range of  $[-1, 1]$ ,  $s^i$  is a learned parameter of the  $i$ -th layer, and  $d^i$  denotes the scaling factor. Because the activation values after the ReLU function are all non-negative, the quantization of activation values will be truncated into the range of  $[0, 1]$ .

##### 4.1. Model Compression

Quantization compresses the original network by reducing the bits of weights [4]. Under extreme constraints, the model can be quantized to binary  $\{-1, +1\}$  to achieve nearly a  $32\times$  model compression ratio [17, 38]. The common way is to train a quantized model in the spatial domain for storage, transmission and calculation, as shown in Fig. 5 (a). A novel idea is proposed, that is, the weights are decomposed into the frequency domain for quantization, storage and transmission. Thus, more information is preserved. In this application, we focus on the quantization of the weights for the classification on ImageNet dataset, and all the activation values are in full-precision form or quantized by the traditional quantizers. Fig. 5 (b) shows the schematic diagram of our method for model compression, where  $\mathbf{W}_{ll}^i$ ,  $\mathbf{W}_{lh}^i$ ,  $\mathbf{W}_{hl}^i$  and  $\mathbf{W}_{hh}^i$  are the multiscale frequency compo-

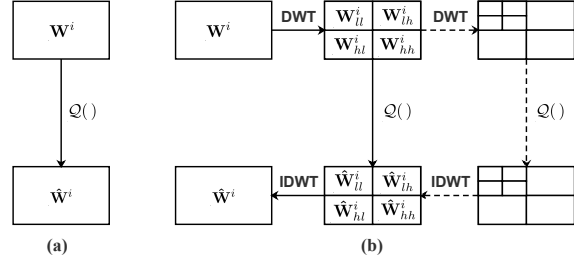


Figure 5: (a) Traditional quantization. (b) Wavelet quantization.

nents decomposed by DWT operation.  $\hat{\mathbf{W}}_{ll}^i$ ,  $\hat{\mathbf{W}}_{lh}^i$ ,  $\hat{\mathbf{W}}_{hl}^i$  and  $\hat{\mathbf{W}}_{hh}^i$  are the quantized multiscale frequency components. We can also perform multi-level decomposition and reconstruction for more detailed quantization, as shown by the dotted line in Fig. 5 (b).

**Experimental results:** The ImageNet dataset (ILSVRC2012) consists of images of 1K categories, and has over 1.2M images in the training dataset and 50K images in the validation dataset. It is a common large-scale dataset for image classification tasks. In order to verify the effectiveness of our method on large-scale datasets and deep networks, we implement experiments with ResNet-18 and ResNet-50 on this dataset. In the experiments, the activation values are in full-precision form or are quantized to 4-bit. Following previous methods [56, 54], we quantize the first convolutional layer and the last fully-connected layer to 8-bit. We apply the pre-trained full-precision model to initialize the quantized model. Network parameters  $\mathbf{W}$  are updated 50 epochs by SGD, the initial learning rate is  $1 \times 10^{-2}$ . The learning rate is decayed by a factor of 10 at epochs 10, 25, and 40, respectively. For ImageNet, the batch size for all the networks is set to 1024. Here, we compare the performance of our method with those of state-of-the-art methods, such as TWN [21], TTQ [55], LQ-Nets [51], QIL [19], DSQ [12], HAQ [46], and HAWQ [8]. HAQ and HAWQ are typical mixed-precision quantization methods.

For each compared method, we report its weight bit, activation value bit, Top-1 accuracy, and weight compression rate. Table 1 shows all the experimental results. We use ‘MWQ [Haar] - [6,2,2,2],  $J=1 - 32$ ’ as an example to explain the result. ‘MWQ’ denotes multiscale wavelet quantization and ‘Haar’ denotes the wavelet base for decomposition. ‘[6,2,2,2],  $J=1$ ’ denotes that the weights are decomposed by single-level wavelet, and the low frequency component is quantized to 6-bit and other high frequency components are quantized to 2-bit. ‘32’ refers to the activation values being in full-precision form. We quantize the weights based on multiple wavelet bases (e.g., *Haar*, *Daubechies*, *Symlets* and *Coiflets*). In Table 1, ‘bd2’ represents the orthogonal *Daubechies* wavelet with approximation order 2. From Table 1, we can see that our method can obtain better classification accuracies than other meth-

Table 1: Accuracy comparisons of ResNet-18 and ResNet-50 on ImageNet. ‘M’ refers to mixed-precision quantization.

Models	Methods	W-Bits	A-Bits	Top-1	W-Comp	
ResNet-18	FP	32	32	70.20	1.00	
	TWN	2	32	65.30	16.00	
	TTQ	2	32	66.60	16.00	
	LQ-Nets	2	32	68.00	16.00	
	MWQ [Haar]	[2,2,2,2], $J=1$		32	<b>68.79</b>	16.00
		[3,2,2,1], $J=1$		32	68.27	16.00
		[4,2,1,1], $J=1$		32	67.41	16.00
		[5,1,1,1], $J=1$		32	67.00	16.00
	LQ-Nets	3	32	69.30	10.67	
	QIL	3	32	69.90	10.67	
	MWQ [Haar]	[3,3,3,3], $J=1$		32	<b>70.04</b>	10.67
		[4,3,3,2], $J=1$		32	69.80	10.67
		[5,3,2,2], $J=1$		32	69.74	10.67
		[6,2,2,2], $J=1$		32	69.43	10.67
		PACT	4	4	69.20	8.00
		LQ-Nets	4	4	69.30	8.00
	DSQ	4	4	69.56	8.00	
	QIL	4	4	70.10	8.00	
	MWQ [Haar]	[4,4,4,4], $J=1$		4	71.01	8.00
	MWQ [db2]	[4,4,4,4], $J=1$		4	71.02	8.00
MWQ [sym2]	[4,4,4,4], $J=1$		4	<b>71.04</b>	8.00	
MWQ [coif2]	[4,4,4,4], $J=1$		4	70.92	8.00	
ResNet-50	FP	32	32	77.15	1.00	
	LQ-Nets	4	4	75.10	8.00	
	HAQ	M	M	75.48	~ 8.00	
	HAWQ	M	M	75.30	~ 8.00	
	MWQ [Haar]	[4,4,4,4], $J=1$		4	76.33	8.00
	MWQ [db2]	[4,4,4,4], $J=1$		4	76.32	8.00
	MWQ [sym2]	[4,4,4,4], $J=1$		4	76.23	8.00
	MWQ [coif2]	[4,4,4,4], $J=1$		4	76.36	8.00
	MWQ [coif2]	[4,4,4,4], $J=2$		4	<b>76.37</b>	8.00

ods. Especially when the activation values are quantized to 4-bit, the accuracies of our method are obviously higher than their full-precision counterparts. When we use different bit-widths to quantize the frequency components of the weights, we find that the experimental results have obvious differences. The high frequency components of the weights also have a great contribution to the quantization effect. When we decompose weights with different wavelets, the experimental results are almost equivalent. Therefore, the decomposition based on multiple wavelet bases is an effective method for model compression.

We take the weights of ‘layer2.0.conv1’ of ResNet-18 for the classification on ImageNet as an example to analyze the numerical distribution of MWQ, the weight statistics histograms are shown in Fig. 6. (a) is the statistics histograms of original weights, (b) is the statistics histograms of quantized 4-bit weights, and (c) is the statistics histograms of quantized 4-bit weights by our method. Obviously, we can see that the weights quantized by our method have more representation states. Therefore, MWQ has stronger representation ability and can achieve better performance under

the same model compression ratio.

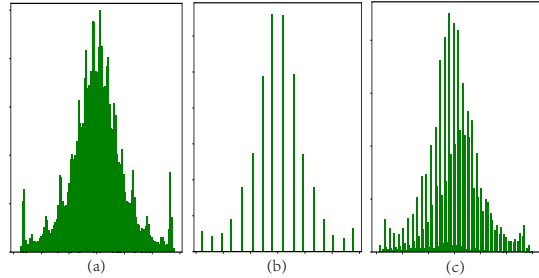


Figure 6: Comparison of weight statistics histograms of ‘layer2.0.conv1’ of ResNet-18 before and after multiscale wavelet quantization. (a) Statistics histogram of original weights. (b) Statistics histogram of original weights after 4-bit quantization. (c) Statistics histogram of data after IDWT reconstruction.

## 4.2. Quantized Network Optimization

Quantized neural network is a typical discrete neural network. The derivative of the quantization function is not defined, and thus traditional gradient optimization methods are not applicable. STE [1] updates gradients by predefining a fixed derivative, which is widely applied in [28, 51, 43]. Experiments and analysis in [22, 35] show that the gradient error caused by quantization and STE greatly harms the accuracy of quantized models when models are quantized to low-bit. DSQ [12] employs a series of hyperbolic tangent functions to gradually approach the staircase function for low-bit quantization. However, it can only be used for the optimization of uniform quantization. Progressive quantization (PQ) [57] uses the high-bit model to initialize the low-bit weights, which can speed up the convergence and improve accuracy.

From the Application 1, we can see that MWQ has stronger representation ability, and provides better performance for quantized networks. Therefore, we use the ideology of PQ for reference and introduce MWQ into the optimization of traditional quantized neural networks. In this application, different from the multistage training pipelines in PQ, we only consider two types of bitwidth precision for weights quantization. In other words, we first train an MWQ model (just like Application 1), and then use the trained model to initialize the target quantized network. As an orthogonal method, our method can support multiple quantizers (e.g., the uniform quantizer and adaptive quantizer). The iterative procedure is shown in Algorithm 1.

**Experimental results:** To verify the effectiveness of our proposed optimization method, we still use the ImageNet dataset to optimize ResNet-18 and ResNet-50 models. We take single-level decomposition by the *Haar* wavelet for MWQ, and the same optimization strategies as in Application 1 are adopted to train a multiscale wavelet quantized model. After 50 epochs, the  $k$ -bit multiscale wavelet quantized model will be used to initialize the parameters of Stage

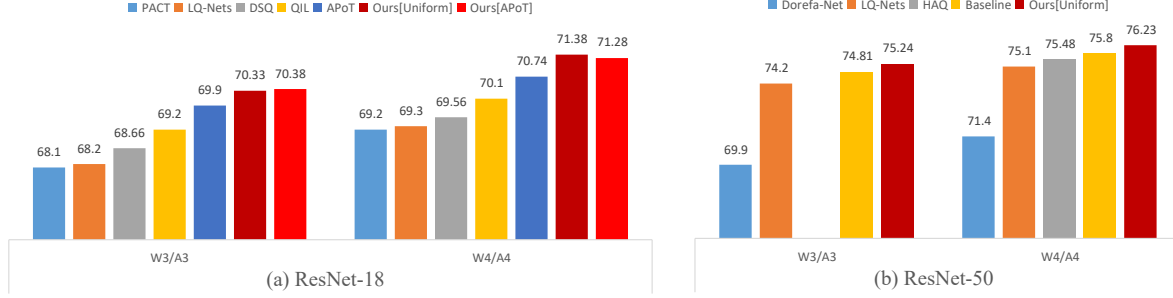


Figure 7: The experimental results of these quantized neural networks based on ResNet-18 and ResNet-50.

---

**Algorithm 1:** Quantized Network Optimization based on Multiscale Wavelet Quantization

---

**Input:** The training dataset  $\{(\mathbf{X}_i, \mathbf{y}_i)\}_{i=1}^N$ ;  
 Initializing parameters by a pre-trained model.

**Output:** A model with weights and activations being quantized into  $k$ -bit.

- 1 **Stage 1:** Training multiscale wavelet quantized model:
- 2 **for**  $epoch = 1, \dots, L$  **do**
- 3     **for**  $t = 1, \dots, T$  **do**
- 4         Quantizing the activations into  $k$ -bit;
- 5         Using Eqs. (8) ~ (10) to quantize the weights into  $k$ -bit;
- 6         Updating weights;
- 7 **Stage 2:** Fine-tuning quantized model:
- 8 Initializing parameters using the trained  $k$ -bit multiscale wavelet quantized model from **Stage 1**;
- 9 **for**  $epoch = 1, \dots, L$  **do**
- 10     **for**  $t = 1, \dots, T$  **do**
- 11         Quantizing the activations into  $k$ -bit;
- 12         Quantizing the weights into  $k$ -bit;
- 13         Updating weights;

---

2. In Stage 2, the initial learning rate is  $1 \times 10^{-3}$  and decayed by a factor of 10 at epochs 20 and 40.

Fig. 7 shows the comparable experimental results on ResNet-18 and ResNet-50. For ResNet-18, we have carried out experiments on two kinds of quantizers (e.g., Uniform and APoT). The two-stage optimization method with MWQ has obvious advantages, and its accuracies are over 70% in 3 bits and 71% in 4 bits. For ResNet-50, we use the trained model by PQ as the baseline (yellow). Compared with baseline, our method is 0.43% higher in 3-bit and 4-bit.

### 4.3. Information Enhancement

In image processing tasks, features (e.g., edges, textures, and shapes) play important roles in image classification, object detection, semantic segmentation, and scene under-

standing. Therefore, it is especially important for image understanding to detect the edge from the small outline of the structure to the boundary of the large visual object. DNNs use multiple hidden layers to achieve feature extraction of images automatically. Due to the lack of supervision on the details of specific regions, the spatial distribution of semantic features will be confused. This phenomenon greatly weakens the representation ability of features and brings difficulties to the construction of hierarchical understanding. SEANet [3] utilizes edge attention to highlight the object and suppress background noise, and SPNet [15] proposes strip pooling to aggregate global and local contexts for scene parsing.

As a tool of multiscale frequency analysis, wavelet can be used for image decomposition. The low frequency component stores the specific information of the image, and the high frequency components store significant information (e.g., edges, textures, and shapes) in different directions. In order to verify the effectiveness of high frequency information and alleviate the loss of spatial information in the process of feature extraction, we consider to decompose the feature maps by wavelet transform and enhance the high frequency information. We introduce scale factors  $\alpha$  into the high frequency components. Fig. 8 illustrates the main process, where  $\mathbf{X}$  and  $\hat{\mathbf{X}}$  denote the original feature map and enhanced feature map, respectively.

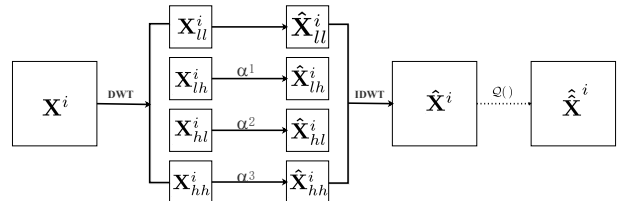


Figure 8: Schematic diagram of information enhancement.

**Experimental results:** We evaluate the proposed information enhancement method for object detection and instance segmentation tasks on the COCO detection benchmark [27], which is one of the most popular large-scale benchmark datasets. This dataset consists of images from 80 different categories. Here, we use the 115K images for

Table 2: Results of Mask R-CNN and its quantized networks by our method on the COCO validation set.

Methods	W/A-Bits	Detection						Segmentation					
		AP	AP <sub>50</sub>	AP <sub>75</sub>	AP <sub>S</sub>	AP <sub>M</sub>	AP <sub>L</sub>	AP	AP <sub>50</sub>	AP <sub>75</sub>	AP <sub>S</sub>	AP <sub>M</sub>	AP <sub>L</sub>
baseline	32/32	40.98	61.53	44.91	24.87	43.87	55.33	37.17	58.60	39.88	18.63	39.49	53.30
Ours [Haar]	32/32	41.27(+0.29)	61.69	45.25	25.05	44.10	53.50	37.42(+0.25)	58.77	40.33	18.90	39.75	53.50
Ours [db2]	32/32	41.31(+0.33)	<b>61.87</b>	45.15	<b>25.30</b>	44.27	53.50	<b>37.50(+0.33)</b>	<b>58.97</b>	<b>40.37</b>	<b>18.98</b>	39.85	53.64
Ours [sym2]	32/32	41.30(+0.32)	61.80	45.10	25.08	44.14	<b>53.88</b>	<b>37.50(+0.33)</b>	58.88	40.29	18.87	39.78	53.69
Ours [coif2]	32/32	<b>41.33(+0.35)</b>	61.79	<b>45.43</b>	25.16	<b>44.28</b>	53.53	37.45(+0.28)	58.96	40.33	18.93	<b>39.89</b>	<b>53.79</b>
baseline	4/4	39.22	59.70	42.50	23.30	42.28	50.84	35.36	56.62	37.68	17.35	37.69	50.58
Ours [Haar]	4/4	39.98(+0.76)	<b>60.43</b>	43.58	<b>24.57</b>	42.83	52.08	<b>36.23(+0.87)</b>	<b>57.55</b>	<b>38.88</b>	<b>18.37</b>	<b>38.46</b>	52.25
Ours [db2]	4/4	39.94(+0.72)	60.42	43.36	23.65	42.76	52.26	36.14(+0.78)	57.51	38.65	17.89	38.28	<b>52.26</b>
Ours [sym2]	4/4	39.96(+0.74)	60.38	43.54	23.48	<b>42.86</b>	<b>52.55</b>	36.02(+0.66)	57.32	38.61	17.67	38.17	51.78
Ours [coif2]	4/4	<b>40.06(+0.84)</b>	60.38	<b>43.71</b>	23.74	42.81	52.32	<b>36.23(+0.87)</b>	57.33	38.83	17.87	38.32	52.21

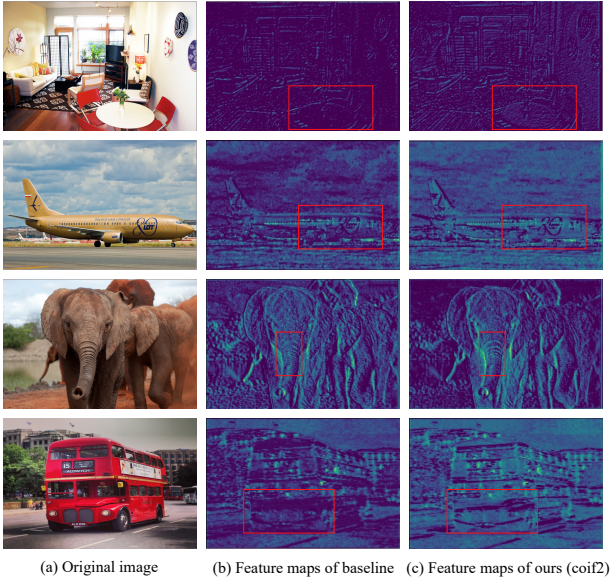


Figure 9: Feature visualization of ResNet-50 in Mask R-CNN.

training and 5K images for validation. We use ResNet-50 as the backbone of Mask R-CNN [14], in which the feature maps are decomposed for information enhancement. *Haar*, *Daubechies*, *Symlets*, and *Coiflets* are applied as wavelet bases to decompose the feature maps. We do experiments on full-precision networks and 4-bit quantized networks. Here, we use Eq. (11) as the quantizer to quantize the weights  $\mathbf{W}$  and enhanced feature maps  $\hat{\mathbf{X}}$ . In the implementation, we apply the pre-trained full-precision model to initialize our model. Our network is fine-tuned with SGD for 100K iterations with the initial learning rate being  $1 \times 10^{-3}$  and the batch size of 16 for 8 V100 GPUs. The learning rate is decayed by a factor of 10 at iterations 20K, 50K, and 80K, respectively. The initial scale factors  $\alpha^i$  are set to 1.2.

We report the standard COCO metrics including AP, AP<sub>50</sub>, AP<sub>75</sub>, AP<sub>S</sub>, AP<sub>M</sub>, and AP<sub>L</sub> in object detection and instance segmentation tasks. Experimental results are shown in Table 2. The results have been significantly im-

proved after enhancing the high frequency information. No matter what kind of wavelet decomposition base is used, the average over IOU thresholds of the full-precision model for detection and segmentation tasks have been improved by more than 0.3 (compared with baseline). For the quantized network, the effect of information enhancement is particularly significant. As can be seen from Table 2, the enhanced networks have significant improvements in terms of the metrics for both tasks (e.g., object detection and instance segmentation) compared with their baselines. Fig. 9 shows the visualization of the feature maps (‘res2’) of quantized backbone (ResNet-50), where (b) shows original feature maps and (c) shows enhanced feature maps by ‘coif2’. The enhancement effect can be clearly seen in the red box.

#### 4.4. Effectiveness Analysis

MWQ contains more operations, and thus it will inevitably require more computation, as shown in Fig. 2. In order to avoid the influence of complex computation on the efficiency of quantized neural networks, we only introduce MWQ in the training process for Applications 1 and 2. Although the compressed model needs only once additional IDWT reconstruction to participate in inference computing, the computation of IDWT is negligible in practical applications. Experiment 3, as an extended application, verified the importance of spatial information (high frequency components), especially in quantized neural networks. Although the multiscale frequency and spatial information of the weights is not interpretable as the activation feature maps, and it also can play an effective role in quantized neural networks.

### 5. Concluding Remarks

In this paper, we proposed a novel quantization method, which considers the spatial information and multiscale information decomposed by wavelet transform. It can alleviate the information loss by matching the appropriate quantization for each frequency component. We verified the effectiveness of the proposed method on model compression, quantized network optimization and information enhancement applications. Due to the flexibility of MWQ,

the discussion in this paper may not be complete, and there are still many innovations and applications (e.g., speech recognition, denoising, and remote sensing image processing) waiting to be explored. In the future, we will use MWQ to train a quantized model that supports multiple bit-widths simultaneously to use in more industrial applications.

## References

- [1] Yoshua Bengio, Nicholas Léonard, and Aaron Courville. Estimating or propagating gradients through stochastic neurons for conditional computation. *arXiv preprint arXiv:1308.3432*, 2013. [2](#), [6](#)
- [2] Zhaowei Cai and Nuno Vasconcelos. Rethinking differentiable search for mixed-precision neural networks. *arXiv preprint arXiv:2004.05795*, 2020. [2](#)
- [3] Xier Chen, Yanchao Lian, Licheng Jiao, Haoran Wang, Yan-Jie Gao, and Shi Lingling. Supervised edge attention network for accurate image instance segmentation. [7](#)
- [4] Yu Cheng, Duo Wang, Pan Zhou, and Tao Zhang. A survey of model compression and acceleration for deep neural networks. *arXiv preprint arXiv:1710.09282*, 2017. [5](#)
- [5] Jungwook Choi, Zhuo Wang, Swagath Venkataramani, Pierce I-Jen Chuang, Vijayalakshmi Srinivasan, and Kailash Gopalakrishnan. Pact: Parameterized clipping activation for quantized neural networks. *arXiv preprint arXiv:1805.06085*, 2018. [2](#)
- [6] Ingrid Daubechies. *Ten lectures on wavelets*. SIAM, 1992. [2](#)
- [7] DDN De Silva, HWMK Vithanage, KSD Fernando, and ITS Piyatilake. Multi-path learnable wavelet neural network for image classification. In *Twelfth International Conference on Machine Vision (ICMV 2019)*, volume 11433, page 1143310. International Society for Optics and Photonics, 2020. [3](#)
- [8] Zhen Dong, Zhewei Yao, Amir Gholami, Michael W Mahoney, and Kurt Keutzer. Hawq: Hessian aware quantization of neural networks with mixed-precision. In *Proceedings of the IEEE International Conference on Computer Vision*, pages 293–302, 2019. [5](#)
- [9] Yiping Duan, Fang Liu, Licheng Jiao, Peng Zhao, and Lu Zhang. Sar image segmentation based on convolutional-wavelet neural network and markov random field. *Pattern Recognition*, 64:255–267, 2017. [3](#)
- [10] EENews. Apple describes 7nm a12 bionic chips. 2018. [1](#)
- [11] Jie Feng, Jiantong Chen, Qigong Sun, Ronghua Shang, Xi-anghai Cao, Xiangrong Zhang, and Licheng Jiao. Convolutional neural network based on bandwise-independent convolution and hard thresholding for hyperspectral band selection. *IEEE Transactions on Cybernetics*, 2020. [2](#)
- [12] Ruihao Gong, Xianglong Liu, Shenghu Jiang, Tianxiang Li, Peng Hu, Jiazhen Lin, Fengwei Yu, and Junjie Yan. Differentiable soft quantization: Bridging full-precision and low-bit neural networks. In *Proceedings of the IEEE International Conference on Computer Vision*, pages 4852–4861, 2019. [2](#), [5](#), [6](#)
- [13] Denis A Gudovskiy and Luca Rigazio. Shiftcnn: Generalized low-precision architecture for inference of convolutional neural networks. *arXiv preprint arXiv:1706.02393*, 2017. [2](#)
- [14] Kaiming He, Georgia Gkioxari, Piotr Dollár, and Ross Girshick. Mask r-cnn. In *Proceedings of the IEEE international conference on computer vision*, pages 2961–2969, 2017. [8](#)
- [15] Qibin Hou, Li Zhang, Ming-Ming Cheng, and Jiashi Feng. Strip pooling: Rethinking spatial pooling for scene parsing. In *Proceedings of the IEEE/CVF Conference on Computer Vision and Pattern Recognition*, pages 4003–4012, 2020. [7](#)
- [16] Huaibo Huang, Ran He, Zhenan Sun, and Tieniu Tan. Wavelet-srnet: A wavelet-based cnn for multi-scale face super resolution. In *Proceedings of the IEEE International Conference on Computer Vision*, pages 1689–1697, 2017. [3](#)
- [17] Itay Hubara, Matthieu Courbariaux, Daniel Soudry, Ran El-Yaniv, and Yoshua Bengio. Binarized neural networks. In *NIPS*, pages 4107–4115, 2016. [2](#), [5](#)
- [18] Qing Jin, Linjie Yang, and Zhenyu Liao. Adabits: Neural network quantization with adaptive bit-widths. *arXiv preprint arXiv:1912.09666*, 2019. [2](#)
- [19] Sangil Jung, Changyong Son, Seohyung Lee, Jinwoo Son, Jae-Joon Han, Youngjun Kwak, Sung Ju Hwang, and Changkyu Choi. Learning to quantize deep networks by optimizing quantization intervals with task loss. In *CVPR*, pages 4350–4359, 2019. [2](#), [5](#)
- [20] Eunhee Kang, Won Chang, Jaejun Yoo, and Jong Chul Ye. Deep convolutional framelet denosing for low-dose ct via wavelet residual network. *IEEE transactions on medical imaging*, 37(6):1358–1369, 2018. [3](#)
- [21] Fengfu Li, Bo Zhang, and Bin Liu. Ternary weight networks. *arXiv preprint arXiv:1605.04711*, 2016. [2](#), [5](#)
- [22] Hao Li, Soham De, Zheng Xu, Christoph Studer, Hanan Samet, and Tom Goldstein. Training quantized nets: A deeper understanding. In *Advances in Neural Information Processing Systems*, pages 5811–5821, 2017. [2](#), [6](#)
- [23] Lingling Li, Liyuan Ma, Licheng Jiao, Fang Liu, Qigong Sun, and Jin Zhao. Complex contourlet-cnn for polarimetric sar image classification. *Pattern Recognition*, 100:107110, 2020. [3](#)
- [24] Qiufu Li and Linlin Shen. Wavesnet: Wavelet integrated deep networks for image segmentation. *arXiv preprint arXiv:2005.14461*, 2020. [3](#)
- [25] Qiufu Li, Linlin Shen, Sheng Guo, and Zhihui Lai. Wavelet integrated cnns for noise-robust image classification. In *Proceedings of the IEEE/CVF Conference on Computer Vision and Pattern Recognition*, pages 7245–7254, 2020. [3](#)
- [26] Yuhang Li, Xin Dong, and Wei Wang. Additive powers-of-two quantization: An efficient non-uniform discretization for neural networks. In *ICLR*, 2019. [2](#)
- [27] Tsung-Yi Lin, Michael Maire, Serge Belongie, James Hays, Pietro Perona, Deva Ramanan, Piotr Dollár, and C Lawrence Zitnick. Microsoft coco: Common objects in context. In *European conference on computer vision*, pages 740–755. Springer, 2014. [7](#)
- [28] Xiaofan Lin, Cong Zhao, and Wei Pan. Towards accurate binary convolutional neural network. In *NIPS*, pages 345–353, 2017. [6](#)

- [29] Mengkun Liu, Licheng Jiao, Xu Liu, Lingling Li, Fang Liu, and Shuyuan Yang. C-cnn: Contourlet convolutional neural networks. *IEEE Transactions on Neural Networks and Learning Systems*, 2020. 3
- [30] Pengju Liu, Hongzhi Zhang, Kai Zhang, Liang Lin, and Wangmeng Zuo. Multi-level wavelet-cnn for image restoration. In *Proceedings of the IEEE conference on computer vision and pattern recognition workshops*, pages 773–782, 2018. 3
- [31] Wei Liu, Qiong Yan, and Yuzhi Zhao. Densely self-guided wavelet network for image denoising. In *Proceedings of the IEEE/CVF Conference on Computer Vision and Pattern Recognition Workshops*, pages 432–433, 2020. 3
- [32] Yunfan Liu, Qi Li, and Zhenan Sun. Attribute-aware face aging with wavelet-based generative adversarial networks. In *Proceedings of the IEEE Conference on Computer Vision and Pattern Recognition*, pages 11877–11886, 2019. 3
- [33] Stephane Mallat. Wavelet signal processing. *preprint*, 1996. 3
- [34] Stephane G Mallat. A theory for multiresolution signal decomposition: the wavelet representation. *IEEE transactions on pattern analysis and machine intelligence*, 11(7):674–693, 1989. 2, 3
- [35] Jeffrey L McKinstry, Steven K Esser, Rathinakumar Appuswamy, Deepika Bablani, John V Arthur, Izzet B Yildiz, and Dharmendra S Modha. Discovering low-precision networks close to full-precision networks for efficient embedded inference. *arXiv preprint arXiv:1809.04191*, 2018. 2, 6
- [36] Daisuke Miyashita, Edward H Lee, and Boris Murmann. Convolutional neural networks using logarithmic data representation. *arXiv preprint arXiv:1603.01025*, 2016. 2
- [37] Nvidia. Nvidia tensor cores. 2018. 1
- [38] Mohammad Rastegari, Vicente Ordonez, Joseph Redmon, and Ali Farhadi. XNOR-Net: Imagenet classification using binary convolutional neural networks. In *ECCV*, pages 525–542, 2016. 2, 5
- [39] Behrouz Alizadeh Savareh, Hassan Emami, Mohamadreza Hajiabadi, Seyed Majid Azimi, and Mahyar Ghafoori. Wavelet-enhanced convolutional neural network: a new idea in a deep learning paradigm. *Biomedical Engineering/Biomedizinische Technik*, 64(2):195–205, 2019. 3
- [40] Hardik Sharma, Jongse Park, Naveen Suda, Liangzhen Lai, Benson Chau, Vikas Chandra, and Hadi Esmaeilzadeh. Bit fusion: Bit-level dynamically composable architecture for accelerating deep neural network. In *ISCA*, pages 764–775. IEEE, 2018. 1, 4
- [41] Qigong Sun, Licheng Jiao, Yan Ren, Xiufang Li, Fanhua Shang, and Fang Liu. Effective and fast: A novel sequential single path search for mixed-precision quantization. *arXiv preprint arXiv:2103.02904*, 2021. 2
- [42] Qigong Sun, Fanhua Shang, Xiufang Li, Kang Yang, Peizhuo Lv, and Licheng Jiao. Efficient computation of quantized neural networks by  $\{-1, +1\}$  encoding decomposition. 2018. 2
- [43] Qigong Sun, Fanhua Shang, Kang Yang, Xiufang Li, Yan Ren, and Licheng Jiao. Multi-precision quantized neural networks via encoding decomposition of  $\{-1, +1\}$ . In *AAAI*, volume 33, pages 5024–5032, 2019. 2, 6
- [44] Harold H Szu, Brian A Telfer, and Shubha L Kadambe. Neural network adaptive wavelets for signal representation and classification. *Optical Engineering*, 31(9):1907–1917, 1992. 3
- [45] Yaman Umuroglu, Lahiru Rasnayake, and Magnus Sjalander. Bismo: A scalable bit-serial matrix multiplication overlay for reconfigurable computing. In *FPL*, pages 307–3077. IEEE, 2018. 1, 4
- [46] Kuan Wang, Zhijian Liu, Yujun Lin, Ji Lin, and Song Han. Haq: Hardware-aware automated quantization with mixed precision. In *CVPR*, pages 8612–8620, 2019. 2, 5
- [47] Shuo-Fei Wang, Wen-Kai Yu, and Ya-Xin Li. Multi-wavelet residual dense convolutional neural network for image denoising. *arXiv preprint arXiv:2002.08301*, 2020. 3
- [48] Travis Williams and Robert Li. Wavelet pooling for convolutional neural networks. In *International Conference on Learning Representations*, 2018. 3
- [49] Bichen Wu, Yanghan Wang, Peizhao Zhang, Yuandong Tian, Peter Vajda, and Kurt Keutzer. Mixed precision quantization of convnets via differentiable neural architecture search. *arXiv preprint arXiv:1812.00090*, 2018. 2
- [50] Jaejun Yoo, Youngjung Uh, Sanghyuk Chun, Byeongkyu Kang, and Jung-Woo Ha. Photorealistic style transfer via wavelet transforms. In *Proceedings of the IEEE International Conference on Computer Vision*, pages 9036–9045, 2019. 3
- [51] Dongqing Zhang, Jiaolong Yang, Dongqiangzi Ye, and Gang Hua. Lq-nets: Learned quantization for highly accurate and compact deep neural networks. In *ECCV*, pages 365–382, 2018. 5, 6
- [52] Qinghua Zhang and Albert Benveniste. Wavelet networks. *IEEE transactions on Neural Networks*, 3(6):889–898, 1992. 3
- [53] Aojun Zhou, Anbang Yao, Yiwen Guo, Lin Xu, and Yurong Chen. Incremental network quantization: Towards lossless cnns with low-precision weights. *arXiv preprint arXiv:1702.03044*, 2017. 2
- [54] Shuchang Zhou, Yuxin Wu, Zekun Ni, Xinyu Zhou, He Wen, and Yuheng Zou. Dorefa-net: Training low bitwidth convolutional neural networks with low bitwidth gradients. *arXiv preprint arXiv:1606.06160*, 2016. 2, 5
- [55] Chenzhuo Zhu, Song Han, Huizi Mao, and William J Dally. Trained ternary quantization. *arXiv preprint arXiv:1612.01064*, 2016. 2, 5
- [56] Bohan Zhuang, Lingqiao Liu, Mingkui Tan, Chunhua Shen, and Ian Reid. Training quantized neural networks with a full-precision auxiliary module. In *Proceedings of the IEEE/CVF Conference on Computer Vision and Pattern Recognition*, pages 1488–1497, 2020. 5
- [57] Bohan Zhuang, Chunhua Shen, Mingkui Tan, Lingqiao Liu, and Ian Reid. Towards effective low-bitwidth convolutional neural networks. In *Proceedings of the IEEE conference on computer vision and pattern recognition*, pages 7920–7928, 2018. 6